Journal of Organometallic Chemistry 695 (2010) 1663–1674

Contents lists available at ScienceDirect

Journal of Organometallic Chemistry

journal homepage: www.elsevier.com/locate/jorganchem

Silyl–substituted germenes. The reactions of germenes generated thermally from acyltris(trimethylsilyl)germane with conjugated enones

Akinobu Naka [a,*], Shinsuke Ueda [a], Hiroki Fujimoto [a], Toshiko Miura [b], Hisayoshi Kobayashi [b,*], Mitsuo Ishikawa [a,*]

[a] Department of Life Science, Kurashiki University of Science and the Arts, Nishinoura, Tsurajima-cho, Kurashiki, Okayama 712-8505, Japan
[b] Department of Chemistry and Materials Technology, Kyoto Institute of Technology, Matsugasaki, Kyoto 606-8585, Japan

ARTICLE INFO

Article history:
Received 31 January 2010
Received in revised form
7 April 2010
Accepted 9 April 2010
Available online 21 April 2010

Keywords:
Germene
Acylpoly(silyl)germane
Thermolysis
Cycloaddition
Germaoxacyclohexene

ABSTRACT

The cothermolysis of pivaloyl- and adamantoyltris(trimethylsilyl)germane (**1** and **2**) with methyl vinyl ketone and acrolein at 120 °C gave the respective six–membered ring compounds, 2-trimethylsiloxy-3,3-bis(trimethylsilyl)-3-germa-1-oxacyclohex-5-ene derivatives, arising from formal [2 + 4] cycloaddition of germenes with enones, along with appreciable amounts of the unchanged starting compounds. Similar thermolysis of **1** and **2** with methyl vinyl ketone and acrolein at 130 °C afforded two types of the products, [2 + 4] cycloadducts and acylbis(trimethylsilyl)germanes arising from the ring-opening reaction of the resulting cycloadducts, respectively. When **1** and **2** were heated in the presence of the same enones at 140 °C, acylbis(trimethylsilyl)germanes were obtained as the main products. The thermolysis of acylbis(trimethylsilyl)germane (**3**) with 2,3-dimethylbutadiene produced two stereoisomers of [2 + 4] cycloadducts. The results of theoretical calculations for the formation of germenes and [2 + 4] cycloaddition of the germenes to enones, and also isomerization of the resulting [2 + 4] cycloadducts, leading to the ring-opened products have also been reported.

1. Introduction

The chemistry of germenes, compounds bearing a germanium–carbon double bond, has been of considerable interest over the past two decades [1–7]. Many types of the germenes, including stable germenes have been synthesized, and their chemical properties have extensively been investigated [8–16]. Thus, the chemical behavior of these germenes toward saturated and unsaturated aldehydes and ketones are well–known. For examples, the reactions of the germenes with saturated nonenolizable aldehydes and ketones afford formal [2 + 2] cycloadducts, while with enolizable carbonyl compounds, the germenes react to give the ene adducts. It has been reported that the reaction of 1,1-dimethylbis(trimethylsilyl)germene with benzophenone affords both [2 + 2] and [2 + 4] cycloadducts, although the [2 + 2] cycloadduct is the predominant species [17]. The reaction of 1,1-dimesitylfluorenylidenegermene with benzaldehyde and benzophenone gives the respective [2 + 2] cycloadducts [18]. Similar reaction of this germene with phenylisocyanate proceeds to give a [2 + 2] cycloadduct, germaoxacyclobutene derivative, arising from addition of the germene to a carbon–oxygen double bond, but not carbon–nitrogen double bond [19]. To verify the mechanism for addition of the germenes to carbonyl compounds, theoretical treatments have also been carried out [20].

Addition reactions of the germenes with conjugated dienes and enones, and their regiochemistry have been investigated. For example, the reaction of 1,1-dimesitylfluorenylidenegermene with 2,3-dimethylbutadiene produces a [2 + 4] cycloadduct [14f], germacyclohexene derivative, while addition of this germene to methyl acrylate, dimethyl maleate, and dimethyl fumarate affords the respective germaoxacyclohexene derivatives, which include a germanium–oxygen bond in the six–membered ring [21].

Recently, we have found that the thermolysis of pivaloyl- and adamantoyltris(trimethylsilyl)germane at 140 °C readily affords the respective silyl–substituted germenes, and the germenes thus formed reacts with 2,3-dimethyl- and 2,3-diphenylbutadiene to give the formal [2 + 4] cycloadducts, germacyclohexene derivatives, in high yields [22]. In order to get more information about

* Corresponding authors.
E-mail addresses: anaka@chem.kusa.ac.jp (A. Naka), kobayashi@chem.kit.ac.jp (H. Kobayashi), ishikawa-m@zeus.eonet.ne.jp (M. Ishikawa).

0022-328X/$ – see front matter © 2010 Elsevier B.V. All rights reserved.
doi:10.1016/j.jorganchem.2010.04.007

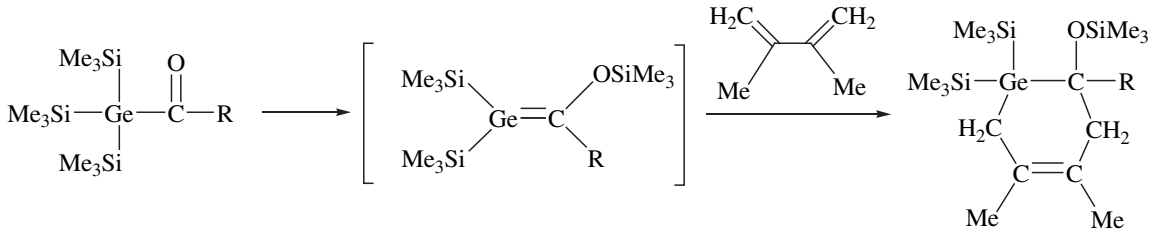

the reactivity of the germenes generated thermally from acylpolysilylgermanes, we investigated the cothermolysis of pivaloyl- and adamantoyltris(trimethylsilyl)germane with methyl vinyl ketone and acrolein under various conditions, and carried out theoretical calculations to clarify the reaction mechanism for these reactions.

2. Results and discussion

We first investigated the thermal reaction of pivaloyltris(trimethylsilyl)germane (**1**) with methyl vinyl ketone. To our surprise, the cothermolysis of **1** with methyl vinyl ketone in a sealed glass tube at 120 °C for 12 h gave 2-*tert*-butyl-6-methyl-2-trimethylsiloxy-3,3-bis(trimethylsilyl)-3-germa-1-oxacyclohex-5-ene (**3**) in 41% yield, along with 32% of the starting compound **1** as shown in Scheme 1. In the reaction of germenes with conjugated enones reported to date, the formation of the [2 + 4] cycloadducts having a Ge–O bond, the 2-germa-1-oxacyclohex-5-ene derivatives has been observed [21]. However, the present reaction proceeded with a different regiochemistry from that of the reactions reported so far, to give a 3-germa-1-oxacyclohex-5-ene derivative, which includes no Ge–O bond (see theoretical calculations shown below). Similar reaction of adamantoyltris(trimethylsilyl)germane (**2**) with methyl vinyl ketone again proceeded to give a germaoxacyclohexene derivative, 2-adamantyl-6-methyl-2-trimethylsiloxy-3,3-bis(trimethysilyl)-3-germa-1-oxacyclohex-5-ene (**4**), in 43% isolated yield, together with 11% of the starting compound **2**. No other volatile products were detected in the reaction mixture, however, nonvolatile substances were detected, when the reaction mixture was treated with a silica gel column for isolation of the product.

The structures of the products **3** and **4** were confirmed by mass, and ^{1}H, ^{13}C, and ^{29}Si NMR spectrometric analysis (see Experimental Section). The mass spectrum of **3** indicates a parent ion at *m*/*z* 448, corresponding to the calculated molecular weight for the germene–methyl vinyl ketone adduct. The ^{13}C NMR spectrum for **3** shows three signals at 0.7, 1.0, and 2.5 ppm, due to the trimethylsiloxy carbons and two different kinds of the trimethylsilyl carbons, and two signals at 4.3 and 113.2 ppm, attributable to the sp^3–hybridized ring carbons, as well as a signal of methyl carbon, two signals of olefinic carbons, and two signals due to the *tert*-butyl carbons. All NMR spectral data obtained for **4** were found to be very similar to those for compound **3**, with the exception of the signals due to the adamantyl group.

The formation of compounds **3** and **4** can be best understood in terms of formal [2 + 4] cycloaddition of the germenes generated thermally from **1** to **2**, to methyl vinyl ketone. Previously, we carried out theoretical calculations concerning the addition reaction of 2-*tert*-butyl- and 2-adamantyl-2-trimethylsiloxy-1,1-bis(trimethylsilyl)silene to propyne and bis(silyl)butadiyne, using density functional theory at the B3LYP/6–31G* level, and demonstrated that the cycloaddition took place in a stepwise manner [23]. Baines et al. also showed experimentally that the reactions of the silenes with alkynes proceeded with the formation of a radical intermediate [24]. In the present reaction, the stepwise process which involves radical species such as **A** shown in Scheme 1, seems to be attractive for the formation of compounds **3** and **4**. Brook et al. have reported that the reactions of silenes produced photochemically from acylpolysilanes with methyl vinyl ketone afford two regioisomers, arising from [2 + 4] cycloaddition, 3-sila-1-oxacyclohex-5-ene and 2-sila-1-oxacyclohex-5-ene in a ratio of 4:1 [25]. The formation of the major product has been explained in terms of predominant frontier orbital interactions.

Escudié and Couret et al. have investigated the reactivity of dimesityl(fluorenylidene)germene toward α–ethylenic aldehyde,

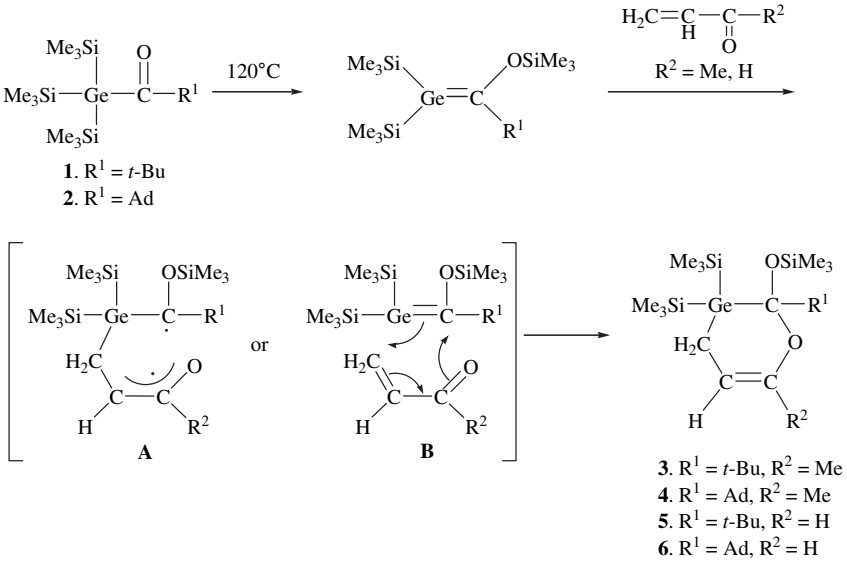

Scheme 1.

ketones, and esters [21b]. They have found that the reactions proceeded to give [2 + 4] cycloadducts, 2-germa-1-oxacyclohex-5-enes, and the regiochemistry in the cycloaddition would be influenced by the well–known oxophilic character of germanium atom and the polarities of the reactants ($Ge^{\delta+}=C^{\delta-}$ and $C^{\delta+}=CC=O^{\delta-}$). Since the electronic property of the present germenes is relatively nonpolar compared to that of dimesitylfluorenylidenegermene, different regiochemistry would be observed in the cycloaddition reaction, giving the products **3** and **4**.

The reactions of **1** and **2** with acrolein also proceeded with the fashion similar to that of the reaction with methyl vinyl ketone. Thus, the thermolysis of **1** with acrolein at 120 °C for 12 h afforded 2-*tert*-butyl-2-trimethylsiloxy-3,3-bis(trimethylsilyl)-3-germa-1-oxacyclohex-5-ene (**5**) in 47% yield. In this reaction, 22% of the starting acylpoly(silyl)germane **1** was recovered unchanged. The reaction of **2** with acrolein under the same conditions gave 2-*tert*-butyl-2-trimethylsiloxy-3,3-bis(trimethylsilyl)-3-germa-1-oxacyclohex-5-ene (**6**) in 57% yield, along with 7% of the starting compound **2**.

Next, we carried out the cothermolysis of **1** and **2** with methyl vinyl ketone at higher temperature, in the hope of obtaining much higher yield of the products. Thus, treatment of **1** with methyl vinyl ketone at 130 °C for 12 h gave two products, six–membered ring compound **3** and pivaloyl[(*Z*)-3-methyl-3-trimethylsiloxy-2-propenyl]bis(trimethylsilyl)germane (**7**), in 29% and 18% yields, respectively. No other volatile products were detected in the reaction mixture. Compound **7** could readily be separated from **3** by column chromatography. The ^{1}H NMR spectrum for **7** shows the presence of the two different kinds of the trimethylsilyl protons at 0.18 and 0.32 ppm, and the methyl proton at 1.68 ppm, in addition to the *tert*-butyl protons at 1.04 ppm, the ring methylene protons at 2.28 ppm, and an olefinic proton at 4.69 ppm. In its ^{13}C NMR spectrum, a signal at 244.9 ppm, due to a carbonyl carbon atom clearly indicates the presence of an acylgermane structure. The ^{29}Si NMR spectrum of **7** reveals two resonances at −6.6 and 15.3 ppm, as expected. These results are wholly consistent with the structure proposed for **7**. Compound **7** is unstable in air, in fact, on exposure to atmospheric oxygen at room temperature, **7** decomposed slowly to give unidentified nonvolatile substances. Similar reaction of **2** with methyl vinyl ketone with 130 °C for 12 h yielded two isomers of the adducts, **4** and adamantoyl[(*Z*)-3-methyl-3-trimethylsiloxy-2-propenyl]bis(trimethylsilyl)germane (**8**) in 23% and 22% yields, respectively. Again, no other volatile products were detected in the reaction mixture. The structure of **8** was verified by spectrometric analysis. As expected, ^{1}H, ^{13}C, and ^{29}Si NMR spectra for **8** show signal patterns very similar to those of **7**, except for the adamantyl group.

Treatment of **1** and **2** with acrolein at 130 °C gave the ring-opened products, together with the [2 + 4] cycloadducts. Thus, when a mixture of **1** and acrolein was heated in a sealed glass tube at 130 °C for 12 h, two products, **5** and pivaloyl[(*Z*)-3-trimethylsiloxy-2-propenyl]bis(trimethylsilyl)germane (**9**) were obtained in 18% and 23% yields, respectively. Similar treatment of **2** with acrolein again gave two products, **6** and adamantoyl[(*Z*)-3trimethylsiloxy-2-propenyl]bis(trimethylsilyl)germane (**10**), in 22% and 32% yields. The structures of the products **9** and **10** were confirmed by mass, and ^{1}H, ^{13}C, ^{29}Si NMR spectrometric analysis (see Experimental Section). Compounds **8**–**10** are also unstable in atmospheric oxygen at room temperature, they decompose slowly to give nonvolatile substances.

The formation of compounds **7**–**10** may be explained by thermal isomerization of the 3-germa-1-oxacyclohex-5-ene derivatives **3**–**6** initially formed by the reaction of the germenes with methyl vinyl ketone and acrolein. Isomerization of **3**–**6** leading to the ring-opened products **7**–**10** presumably involves a 1,3-trimethylsilyl shift to the oxygen atom in the six–membered ring, and simultaneous bond migration, as shown in Scheme 2. As discussed below, theoretical treatments for isomerization of the 3-germa-1-oxacyclohex-5-enes **3**–**6** to the ring-opened products **7**–**10** clearly indicate that the isomerization proceeds with a concerted process (see TS-6 in Fig. 3). In addition, the calculations using the real model show that the ring-opened product (LM-7) is energetically more stable than the six–membered cyclic compound (LM-6), as shown in Figs. 7(b) and 8(b).

At 140 °C, compound **1** reacted with methyl vinyl ketone to give the ring-opened product **7** in 41% yield, as the sole volatile product, together with appreciable amounts of nonvolatile substances. Similar treatment of **2** with methyl vinyl ketone afforded compound **8** in 29% yield, along with the nonvolatile products. In this reaction, a small amount of **4** (4% yield) was also isolated. As expected, the reaction of **1** and **2** with acrolein at 140 °C afforded the ring-opened products **9** and **10**, as the major products (see Experimental Section).

To learn whether or not the ring-opened products **7**–**10** come from isomerization of the 3-germa-1-oxacyclohex-5-enes **3**–**6**, we carried out the thermolysis of **3**. Thus, when compound **3** was heated at 140 °C for 12 h in a sealed glass tube, **7** was obtained in 43% yield, as the sole volatile product, indicating that the 3-germa-1-oxacyclohex-5-ene **3** isomerized to give the ring-opened product **7** under the conditions used (Scheme 3).

The low yields of the product **7**–**10** may be ascribed to their thermal instability. In fact, when the thermolysis of **3** was carried

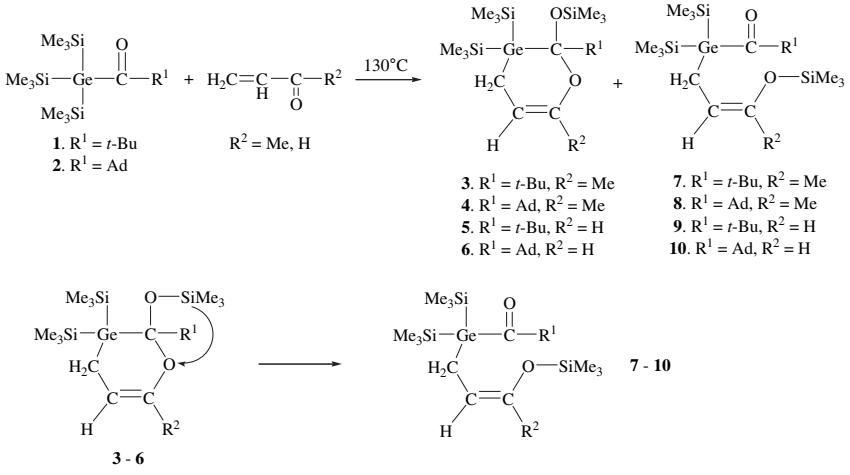

Scheme 2.

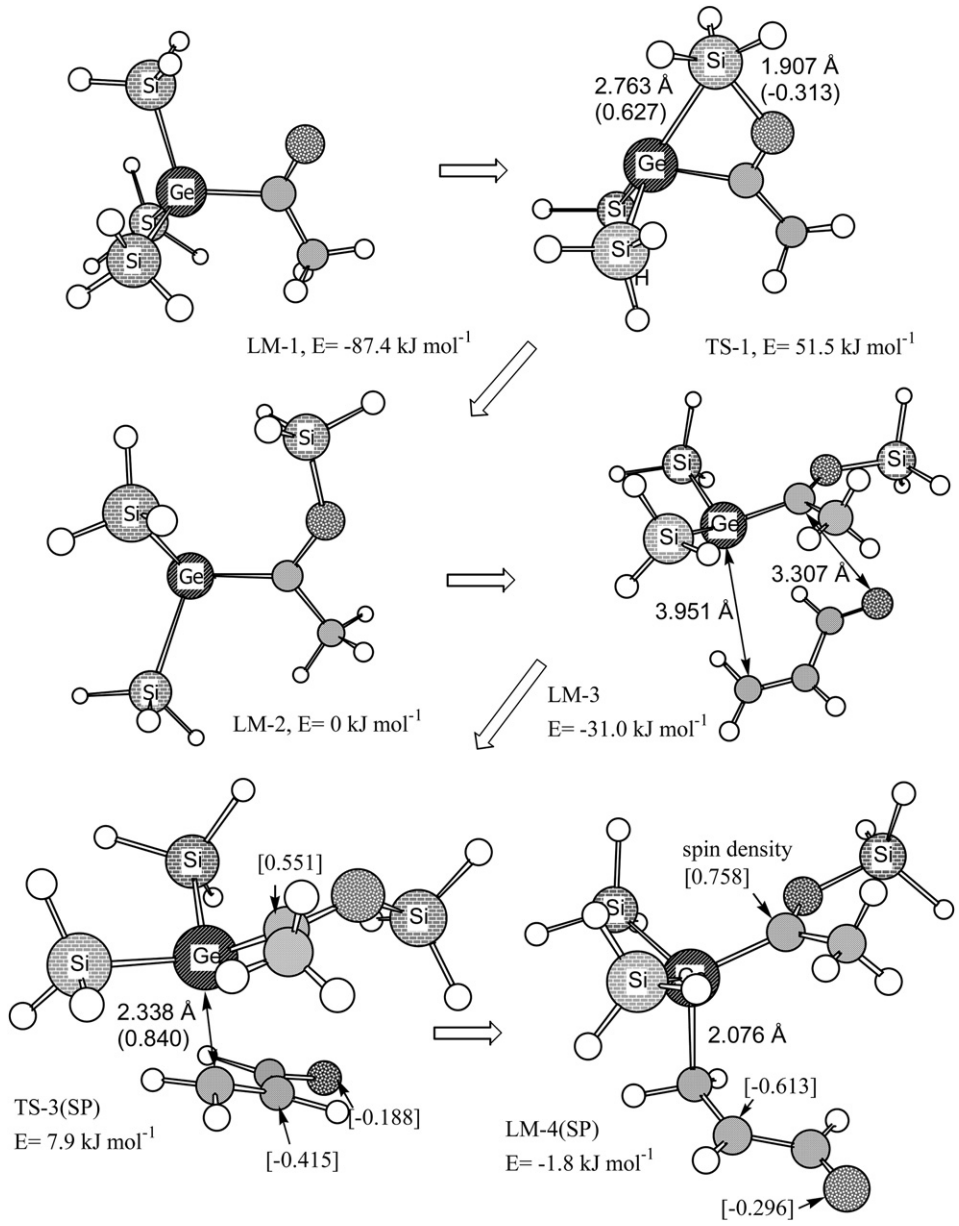

Fig. 1. Optimized structures for LM-1, TS-1, LM-2, LM-3, TS-3(SP), and LM-4(SP) with simplified models along the reaction path described by Scheme 1. Concerted route with the *s-trans* conformer of acrolein. "(SP)" means the spin polarized solution.

out in the presence of 2,3-dimethyl-1,3-butadiene at 140 °C for 24 h, two stereoisomers of [2 + 4] cycloadducts, compounds **11** and **12** were obtained in 92% yield in a ratio of 1:1. The formation of the products **11** and **12** may be best understood in terms of the formal [2 + 4] cycloaddition of the germenes arising from a 1,3-shift of a trimethylsilyl group on the germanium atom to the carbonyl oxygen in **7** with butadiene as shown in Scheme 4. Compounds **11** and **12** thus obtained are unstable toward atmospheric oxygen, and they decompose slowly to give the unidentified nonvolatile substances in the air.

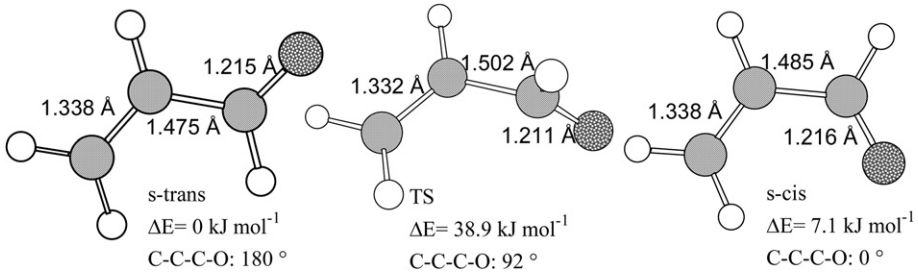

Fig. 2. Optimized structures for s-trans, TS, and s-cis conformation of acrolein. The relative energy, the C–C and C-O bond lengths and the C-C-C-O dihedral angle are shown.

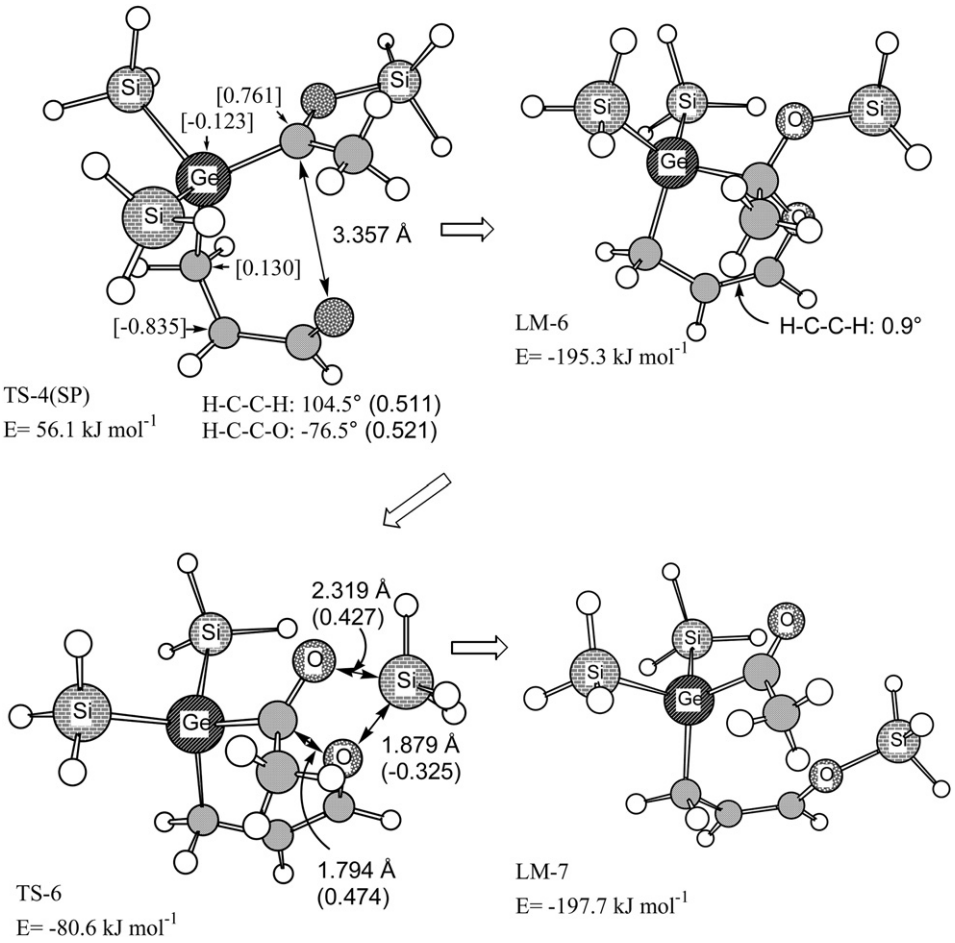

Fig. 3. Optimized structures for TS-4(SP), LM-6, TS-6, and LM-7 with simplified models along the reaction path described by Schemes 1 and 2. Stepwise route with the *s-trans* conformer of acrolein. "(SP)" means the spin polarized solution.

The thermolysis of **1** and **2** with crotonaldehyde and cinnamaldehyde at 120–140 °C gave no addition products, but produced nonvolatile products. Presumably, the presence of bulky substituents on both the reactants and the substrates prevents to the formation of the [2 + 4] cycloadducts.

2.1. Theoretical calculations

To obtain some information concerning the energy and structure changes for the reaction of acylgermanes **1** and **2** with enones, leading to the products **3**–**6** and **7**–**10,** theoretical calculations based on the density functional theory (DFT) method were employed. The calculations were performed in two models. In real models, the molecular structures are identical with those used in the experiments, whereas all methyl groups for **1** were replaced by the hydrogen atoms in simplified models. All local minima and transition states (TS's) were characterized with the simplified models. At the TS, the intrinsic reaction coordinate (IRC) analysis [26] was carried out for both directions. The IRC calculation was restricted in the neighborhood of the TS. At the end point, the IRC was followed by normal optimization runs to confirm the continuity of the reaction coordinate to the preceding and succeeding local minima. As shown below, both spin restricted (spin symmetric) solution and the spin polarized (broken symmetry) solution were obtained for a part of the reaction coordinate.

Local minima and TS's relating to the Ge-C bond formation were reevaluated with the real models. The initial structures of the real models were constructed by replacing the hydrogen atoms in the simplified models of optimized structures with the methyl groups. The calculations were carried out with the hybrid B3LYP method [27,28] and the 6–31G(d) basis sets, which were implemented in the Gaussian 03 software [29].

Fig. 1 shows the reaction profile for the formation of a germene, followed by addition of the resulting germene to an enone, as indicated in Scheme 1. LM-1 is a simplified form of **1**, and LM-2 is a germene derived from LM-1, and TS-1 is the TS located between them. The bond lengths for some typical bonds in TS-1, LM-3, TS-3 (SP), and LM-4(SP) are shown in Fig. 1. In the structures of TS's, the number in parentheses indicates the weight of the geometrical parameter (such as bond length) in direction of the reaction coordinate. (We represent the reaction coordinate in terms of bond lengths, bond angles and dihedral angles. To confirm that the TS obtained is what we are seeking, it is essentially important that the dissociating or forming bond has a major weight among the geometrical parameters). For example, elongation of the Ge–Si bond (0.627) for TS-1 is the major factor to characterize this TS, and shortening of the Si–O bond (−0.313) is the second factor. This deformation of the structure leads to LM-2, and the opposite deformation returns to LM-1.

We have examined two configurations of acrolein, *s*-trans and *s*-cis for the addition reaction. Their LM and TS structures are shown in Fig. 2q. The *s*-cis confomer is unstable than the *s*-trans confomer only by 7 kJ mol^{-1}, but they are separated by a barrier of 39 kJ mol^{-1}. First we treated the reaction of the germene with the *s*-trans conformer of acrolein. LM-3 is the optimized structure consisting of LM-2 and *s*-trans acrolein, which is more stable by

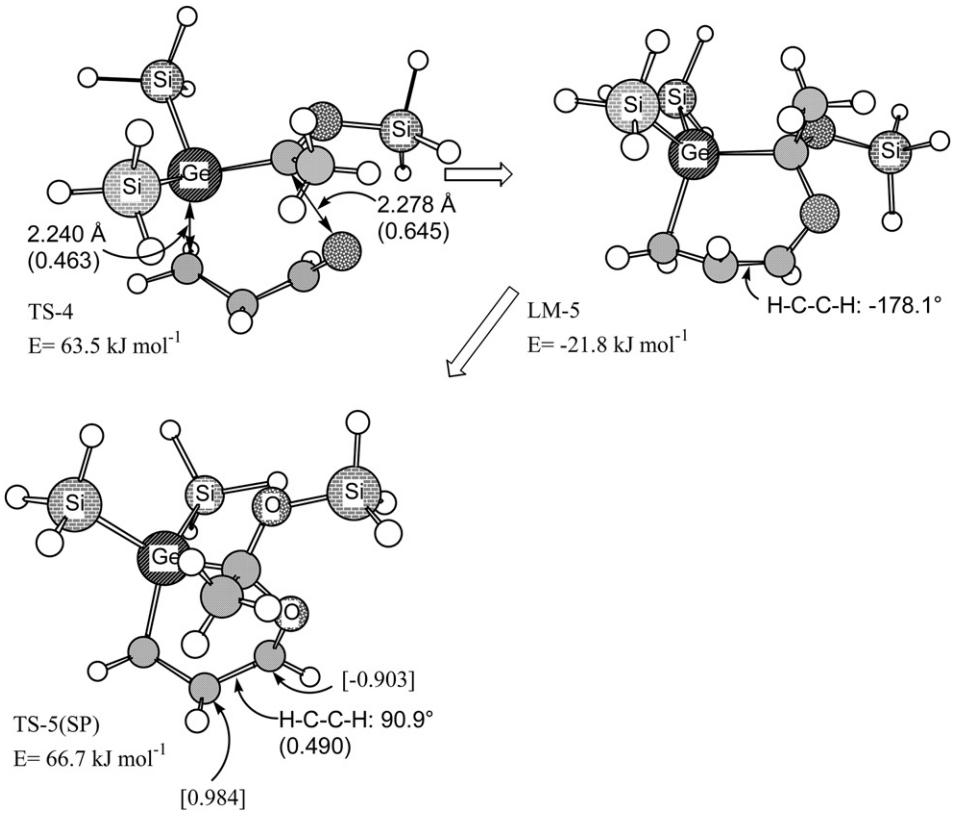

Fig. 4. Optimized structures for TS-4, LM-5, and TS-5(SP) with simplified models along the reaction path described by the Scheme 1. Unique structures in the concerted route with the *s-trans* conformer of acrolein. TS-5(SP) is the TS for the trans-cis conversion of configuration of acrolein moiety, and has a spin polarized solution.

31 kJ mol^{-1} than the two isolated molecules. The energetics along the reaction is compiled in Figs. 7 and 8, and will be discussed later.

In the reaction path from LM-3 to LM-6, two reaction routes were considered. One of them is a stepwise process where the Ge—C bond is formed first, and other involves a concerted process, in which the Ge—C and C—O bonds are formed simultaneously. The structures of TS-3(SP) and LM-4(SP), which are characterized only by the spin polarized calculations, are also shown in Fig. 1. In these structures, some remarkable spin densities are shown in square brackets. TS-3(SP) is the TS for the Ge—C bond formation. The largest α spin density accumulates on the C atom adjacent to the Ge atom. The largest β spin density for the acrolein moiety accumulates on the C atom which is the nearest neighbor to the bond forming C atom. However, the second largest β spin density accumulates on the O atom, which implies formal [2 + 4] cycloaddition. LM-4(SP) is the local minimum, in which the Ge—C bond is formed first, but the C—O bond is not yet.

The structures of TS's and local minima for the latter half of stepwise addition are shown in Fig. 3. TS-4(SP) is not directly the TS for the formation of the C—O bond, but the TS for the internal rotation from *s*-trans to *s*-cis conformation of the acrolein moiety. The reaction coordinate localizes in the change of dihedral angles such as H—C—C—O and H—C—C—H. The IRC analysis to the forward direction and the successive optimization calculation lead to LM-6 with the formation of the C—O bond. The resulting LM-6 is the simplified model for **3**—**6**. In the transformation of LM-6 to LM-7 via TS-6, a 1,3—shift of the H_3Si group on the siloxy oxygen to the ring oxygen in LM-6 and simultaneous C—O bond scission in the six—membered ring are involved, and the acylsilane derivative LM-7, the simplified model for **7**—**10**, is formed. This is the lowest energy pass of the reaction.

Fig. 4 shows the TS's and local minima involved in the concerted process. Starting from LM-3, TS-4 is the TS for the simultaneous formation of the Ge—C and C—O bonds. However, in the resulting LM-5, two H atoms on the sp^2—hybridized carbon atoms in the acrolein moiety are located in a trans fashion, and LM-5 is different from **3**—**6** shown in Scheme 1. In order to produce a simplified model for **3**—**6**, the trans configuration of two H atoms on the sp^2—hybridized carbons in LM-5 must be converted to the cis configuration. TS-5(SP) is the TS, where the dihedral angle H-C-C-H is 91°. This structure is obtained only by the spin polarized solution, and has a biradical character. The structure of LM-6 formed via TS-5 (SP) is the same as that obtained by the stepwise process. Thus the concerted process includes the spin polarized solution, TS-5(SP) which is the highest energy on the reaction coordinate.

Next we considered the reaction profile for cycloaddition, leading to a product including the Ge-O bond formed by the inverse addition of s-trans acrolein to the germene. Fig. 5 shows the structures and relative energies from LM-3-inv through TS-5-inv (SP). The suffix "inv" indicates the inverse addition of acrolein. LM-3-inv is the reactant where the germene and acrolein interact weakly. TS-3-inv(SP) is the TS for the Ge-O bond formation, and a resulting local minimum is LM-4-inv(SP). Similar to the process for the formation of the Ge-C bond (normal addition) in the reaction of the germene with s-trans acrolein shown in Fig. 3, the reaction coordinate with the lowest energy includes the internal rotation of the acrolein moiety, and TS-4-inv(SP) is the TS. This energy is 73 kJ mol^{-1} and considerably higher than that for TS-4 (SP), 56 kJ mol^{-1}. Unlike the normal addition, the reaction coordinate from TS-4(SP) does not afford a six-membered product, like LM-6, but gives LM-5-inv(SP). LM-6-inv is produced from LM-5-inv (SP) via TS-5-inv(SP) with a slight low barrier (4 kJ mol^{-1}), as shown in Fig. 6.

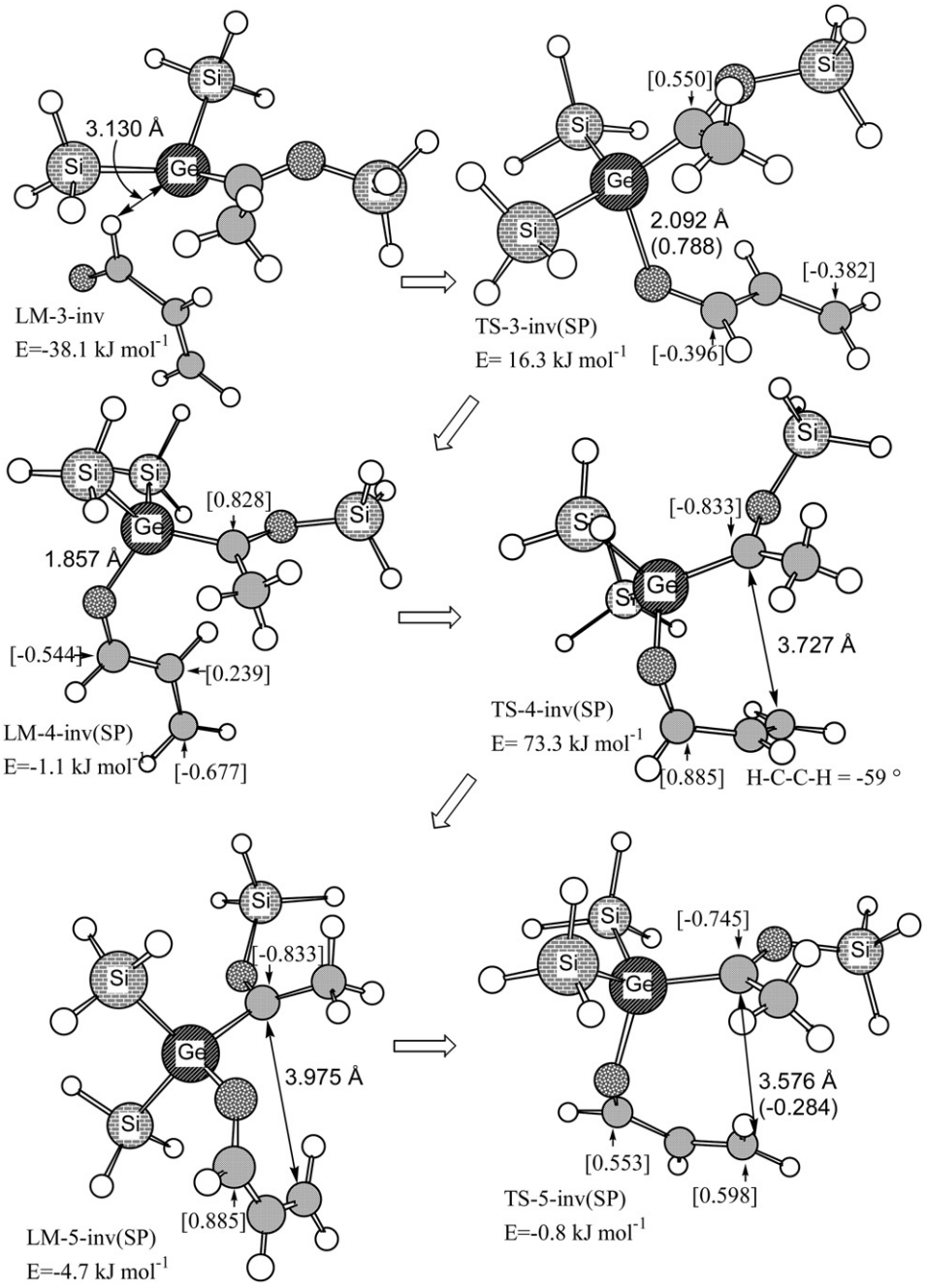

Fig. 5. Optimized structures for LM-3-inv, TS-3-inv(SP), LM-4-inv(SP), TS-4-inv(SP), LM-5-inv(SP), and TS-5-inv(SP) with simplified models along the stepwise inverse addition with the *s*-trans conformer of acrolein. TS-5-inv(SP) connects to LM-6-inv, which is shown in Fig. 6. "inv" and "(SP)" mean the inverse addition and the spin polarized solution.

Then we considered the reaction profile for the cycloaddition of the germene with the *s*-cis conformer of acrolein. The unique structures different from those with the *s*-trans conformer, LM-3c and TS-4c were found, as shown in the upper part of Fig. 6. (The suffix "c" is used to discriminate the structures from those related to *s*-trans conformer.) LM-3c is less stable by 7 kJ mol^{-1} than LM-3, which is an energy difference between the *s*-cis and *s*-trans conformers. (The reference energy is a sum of energies of the germene and *s*-trans conformer of acrolein throughout the work.) TS-4c is the TS for the simultaneous formation of the Ge—C and C—O bonds, and it locates between LM-3c and LM-6. Obviously the trans-cis conversion after cycloaddition does not exist. In the reaction with the *s*-cis conformer, only the concerted process is possible to occur, and therefore the LM's and TS's for the stepwise addition are not characterized. The lower part of Fig. 6 shows the unique structure found in the course of cycloaddition of the germene and s-cis acrolein to give the product having the Ge-O bond. Similar to the normal addition, only the concerted process is characterized. LM-6-inv is a common product between the stepwise and concerted processes, and much stabilized compared to the normal addition product, LM-6, probably due to the presence of a polar Ge-O bond.

All energies calculated for the simplified and real models are shown in Figs. 7(a)(b) and 8(a)(b). Energetic differences between the Ge-C and Ge-O bond formation in the normal and inverse addition of acrolein to the germene are discussed with the simplified models. Then the energetic differences between the stepwise and concerted reaction are compared using the real models. Fig. 7(a) shows three

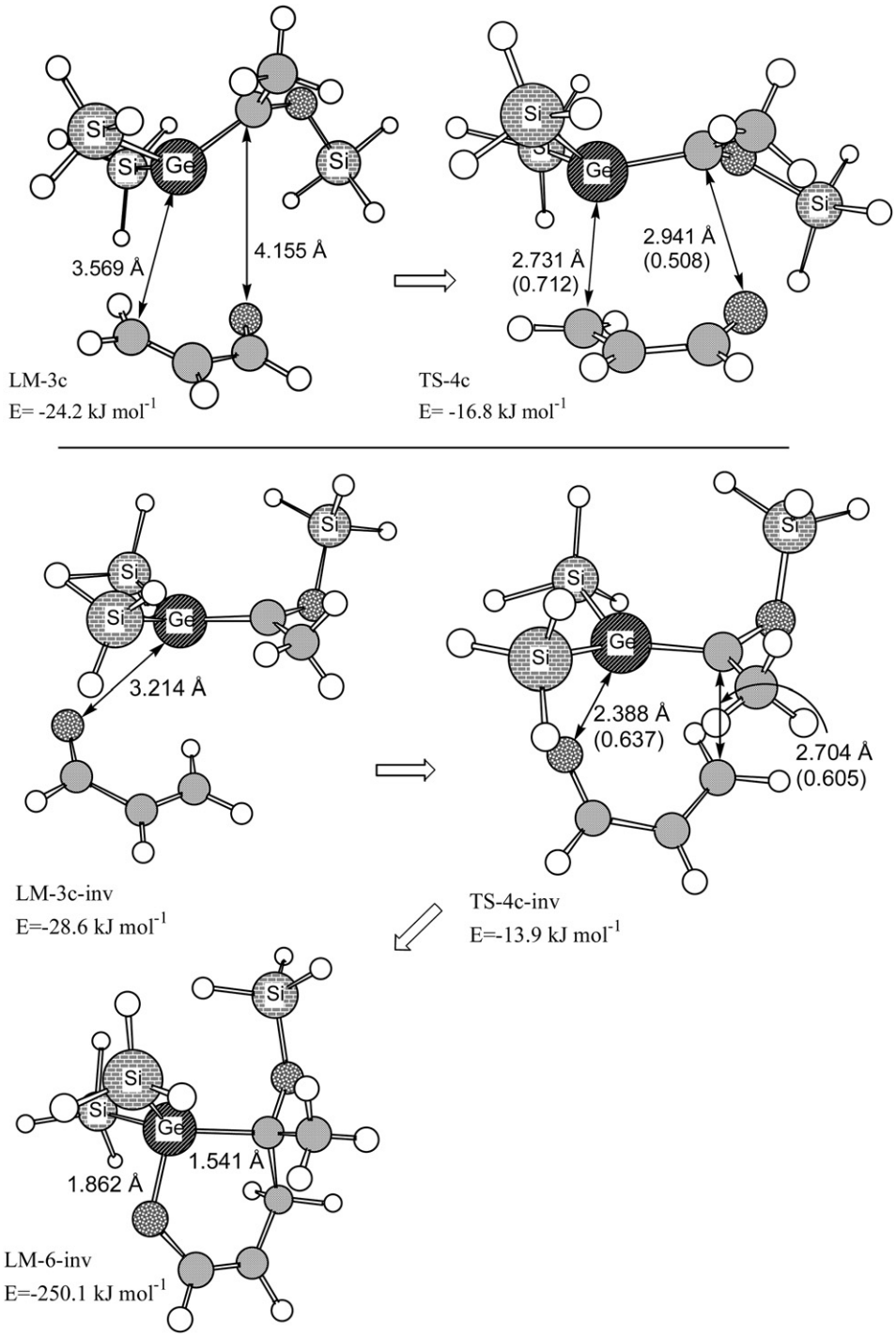

Fig. 6. Optimized structures for LM-3c, TS-4c, LM-3c-inv, TS-4c-inv, and LM-6-inv with simplified models, which are the structures formed from the *s*-cis conformer of acrolein in the concerted process. LM-3c and TS-4c may exist along the reaction path described by Scheme 1, and LM-3c-inv, TS-4c-inv are the counterparts of the formers. "inv" means the inverse addition.

normal addition reactions and one inverse addition reaction of the germene with s-trans conformer of acrolein. The spin restricted solution leads up to LM-5, but the spin polarized solution (polarized-2) is necessary to represent the internal rotation to s-cis confomer. In the spin polarized solution (polarized-1), this internal rotation can occur before the O-C bond formation around TS-4(SP) and the successive reaction coordinate directly leads to LM-6. This reaction pathway is energetically the lowest.

The energies for TS's and LM's in the inverse addition reaction correspond well to those in the normal addition reaction, and are plotted on the same graph. The largest difference is seen at TS-4(SP) and TS-4-inv(SP), and their relative energies are 56 and 73 kJ mol^{-1}. This is the reason why the product with the Ge-O bond is not formed although LM-6-inv is more stable than LM-6 by 55 kJ mol^{-1}. The reaction from LM-6 to LM-7 is common to all routes and well represented by the concerted mechanism.

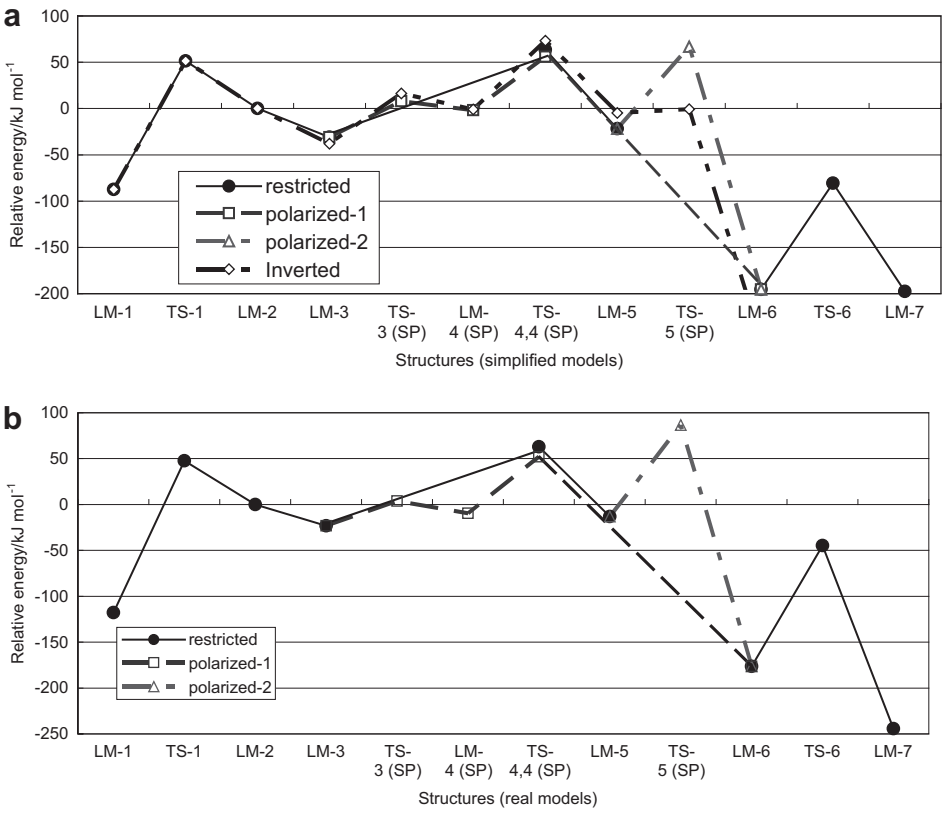

Fig. 7. Energy profile from LM-1 to LM-7 along the reaction path described by Schemes 1 and 2 with (a) simplified, and (b) real models. The energies from TS-3(SP) to TS-5(SP) are unique parts for the *s*-trans conformation of acrolein. The sum of energies of LM-2 and isolated *s*-trans conformer of acrolein is taken as the reference, and all the energies plotted are relative values for this reference. Spin restricted and spin polarized solutions are plotted as "restricted" and "polarized" on the same graph, and then the label on the abscissa is a generic name. For example, "TS-4,4(SP)" represents "TS-4, or TS-4(SP), or "TS-4-inv(SP)".

Fig. 7(b) shows the energetics for three normal addition using the real models. For a 1,3-silyl shift in LM-1 leading to LM-2, the latter is destabilized by 118 kJ mol^{-1}, and the activation energy of TS-1 measured from LM-1 is 166 kJ mol^{-1}, the largest barrier on the reaction coordinate. (The energy for LM-2 is zero since we adopted the sum of energies of germene and *s*-trans acrolein as the zero of relative energy.) In the addition reaction of *s*-trans acrolein to LM-2, LM-3 is produced, whose energy is stabilized by 23 kJ mol^{-1} compared to two isolated molecules. The concerted and stepwise process for this reaction should be compared in more detail. In the concerted process, LM-3 is followed by TS-4, and then LM-5, which can not be identified as a correct structure experimentally. In order to convert two H atoms located in a trans fashion on the sp^2—hybridized carbon atoms in the acrolein moiety of TS-5(SP) to a cis-fashion, the carbon—carbon double bond must be cleaved. This involves the radical scission of the carbon—carbon double bond in TS-5(SP), and needs the highest activation energy. On the other hand, the conformation change from *s*-trans to *s*-cis is facile through TS-4(SP), and the stepwise process directly leads to LM-6 with cis configuration. TS-6 is the TS for the ring-opening reaction, and it proceeds with the energy below zero to give LM-7. The final product, LM-7 is more stable than LM-5, arising from the reaction of LM-1 and *s*-trans acrolein by 126 kJ mol^{-1}. On the basis of the results described above, the concerted route from LM-3 to LM-7 may be possible to proceed, but it is less realistic from the viewpoint that trans-cis conversion in the acrolein moiety has the highest energy on the reaction coordinate.

The energy profile for the cycloaddition of the germene with *s*-cis acrolein is shown in Fig. 8(a)(b). Fig. 8(a) shows the energetics for the normal and inverse addition reaction with the simplified models. The energy of LM-3c derived from *s*-cis acrolein is lower than that of LM-3 from *s*-trans by 7 kJ mol^{-1}, whereas *s*-cis acrolein is unstable than *s*-trans acrolein by 7 kJ mol^{-1}. This means that the interactions between germene and acrolein are strengthened with the *s*-cis conformation. TS-4c is the TS for the concerted cycloaddition, and its energy is lower than those for TS-1, TS-4 and TS-4 (SP). Therefore, in the cycloaddition with *s*-cis acrolein, the highest activation barrier shifts to the energy for TS-1, and the energy profile becomes down hill after the formation of germene. The energetics for the inverse addition is almost the same as that for the normal addition except that LM-6-inv is more stable than LM-6. This means that both products including the Ge-C and Ge-O bonds are formed by the reaction with the s-cis conformer of acrolein. This point contradicts with the experimental results, and therefore we assume that the concentration of the s-cis conformer of acrolein is lower than that of the s-trans. The fact that a barrier of 39 kJ mol^{-1} is required for conversion of the s-trans conformer to s-cis may support this assumption. The energetics for the normal addition reaction with the real models is shown in Fig. 8(b), and this reaction profile is almost identical with that of the simplified models.

In conclusion, the thermolysis of acylpoly(silyl)germanes **1** and **2** with methyl vinyl ketone and acrolein at 120 °C proceeded to afford the formal [2 + 4] cycloadducts, arising from addition of the germenes produced thermally from acylpoly(silyl)germane to vinylketones. At 130 °C, however, **1** and **2** reacted with methylvinylketone and acrolein to afford the [2 + 4] cycloadducts and the ring-opened acylgermane derivatives, arising from a 1,3-silyl shift on the siloxy oxygen to the ring oxygen, respectively. Similar reactions at 140 °C gave the ring-opened acylgermanes as the main products.

The theoretical calculations based on the DFT methods characterized the LM's and TS's locating on the reaction coordinate starting from **1**, through **5** to **9**. Both the simplified and real models gave almost the same energy profiles. The [2 + 4] cycloaddition was

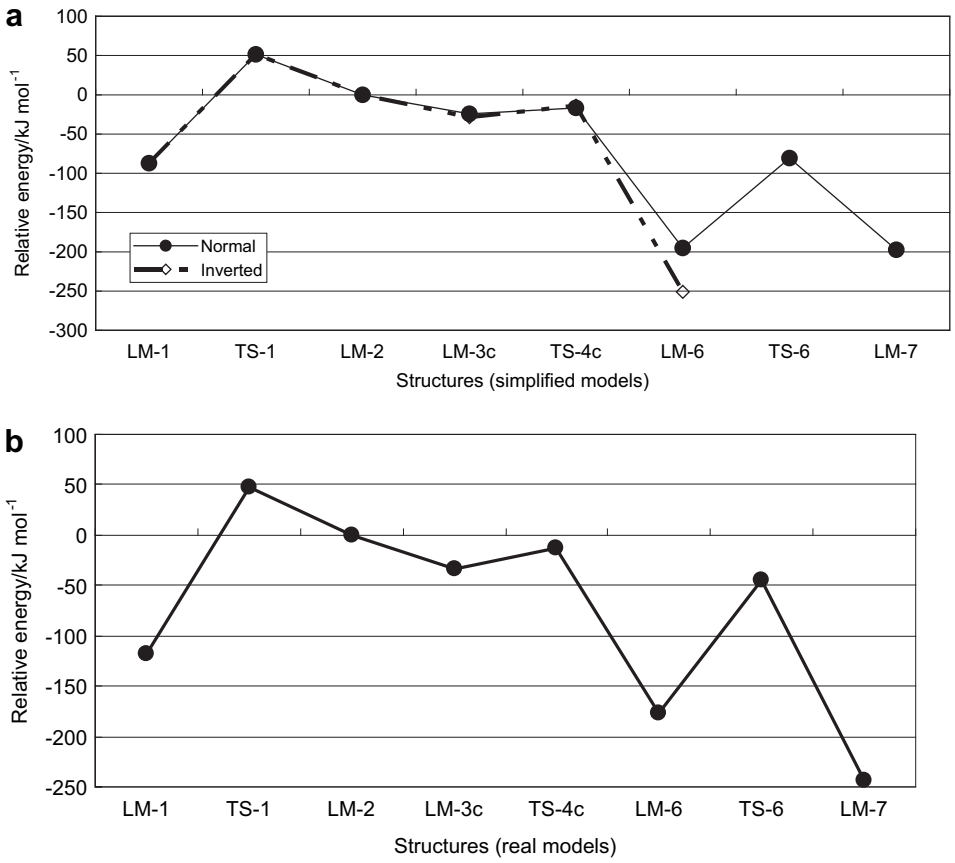

Fig. 8. Energy profile from LM-1 to LM-7 along the reaction path described by Schemes 1 and 2 with (a) simplified, and (b) real models. The energies for LM-3c and TS-4c are unique parts for the *s*-cis conformation and the normal addition of acrolein. For the *s*-cis conformation and the inverse addition, the energies for LM-3c-inv and TS-4c-inv are unique parts, and they are also plotted on the corresponding label of the abscissa in (a).

examined with the spin restricted and spin polarized solutions. The calculations indicated that the stepwise process is energetically more favorable for the cycloaddition of the germene with *s*-trans acrolein than that of the concerted process. With *s*-cis acrolein, only the concerted process is operative, and it is energetically facile reaction path for the formation of both products including the Ge-C and Ge-O bond. Eventually, we conclude that cycloaddition of the germene with acrolein proceeds through the stepwise process with *s*-trans acrolein.

3. Experimental

3.1. General Procedure

All reactions of acylpolysilylgermanes were carried out in a degassed sealed glass tube (1.0 cm × 15 cm). Yields of the products were calculated on the basis of the isolated products. NMR spectra were recorded on JNM-LA300 spectrometer and JNM-LA500 spectrometer. Low– and high–resolution mass spectra were measured on a JEOL Model JMS–700 instrument. Melting point was measured with a Yanaco–MP–S3 apparatus. Column chromatography was performed by using Wakogel C-300 (WAKO).

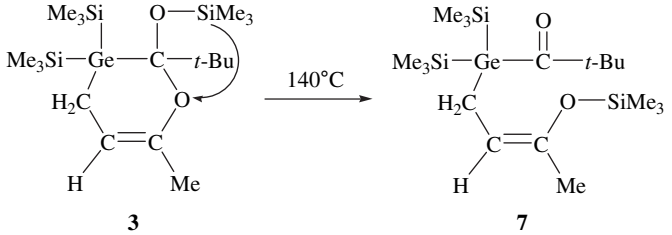

3 **7**

Scheme 3.

3.2. Reaction of ***1*** with methyl vinyl ketone at 120 °C

A mixture of compound **1** (0.1290 g, 0.342 mmol) and 0.0750 g (1.07 mmol) of methyl vinyl ketone was heated in a sealed tube at 120 °C for 12 h. Product **3** (0.0632 g, 41% isolated yield) and the starting compound **1** (0.0420 g, 32%) were isolated by column chromatography. For **3**: Anal. Calcd for $C_{18}H_{42}O_2Si_3Ge$: C, 48.32; H, 9.46. Found: C, 48.24; H, 9.83. MS *m*/*z* 448 (M^+); ^{1}H NMR δ (C_6D_6) 0.247 (s, 9H, Me_3Si), 0.253 (s, 9H, Me_3Si), 0.27 (s, 9H, Me_3Si), 1.10 (s, 9H, *t*-Bu), 1.33 (dd, 1H, CH_2, J = 15.3 Hz, 8.6 Hz), 1.70 (br s, 3H, Me), 1.75 (br d, 1H, CH_2, J = 15.3 Hz), 4.68 (br d, 1H, olefinic proton, J = 8.6 Hz); ^{13}C NMR δ (C_6D_6) 0.7, 1.0, 2.5 (Me_3Si), 4.3 (CH_2Ge), 22.4 (Me), 26.8 (Me_3C), 40.6 (CMe_3), 96.7 (C=C), 113.2 (CO), 149.9 (C=C); ^{29}Si NMR δ (C_6D_6) −8.5, −7.8, 7.4.

3.3. Reaction of ***2*** with methyl vinyl ketone at 120 °C

A mixture of compound **2** (0.1233 g, 0.271 mmol) and 0.0801 g (1.14 mmol) of methyl vinyl ketone was heated in a sealed tube at 140 °C for 12 h. Product **4** (0.0609 g, 43% isolated yield) and the starting compound **2** (0.0133 g, 11%) were isolated by column chromatography. For **4**: Anal. Calcd for $C_{24}H_{48}O_2Si_3Ge$: C, 54.85; H, 9.21. Found: C, 54.48; H, 9.01. Mp. 123–125 °C; MS *m*/*z* 526 (M^+); ^{1}H NMR δ (C_6D_6) 0.27 (s, 9H, Me_3Si), 0.28 (s, 9H, Me_3Si), 0.30 (s, 9H, Me_3Si), 1.33

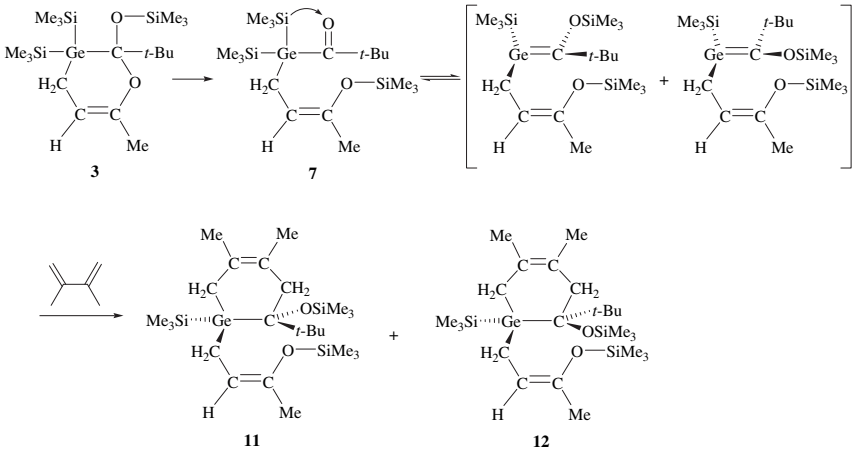

Scheme 4.

(dd, 1H, CH_2, J = 14.9 Hz, 8.4 Hz), 1.70–2.03 (m, 19H, Ad, Me, CH_2), 4.69 (d, 1H, olefinic proton, J = 8.4 Hz); ^{13}C NMR δ (C_6D_6) 0.8, 1.1, 2.6 (Me_3Si), 4.0 (CH_2Ge), 22.3 (Me), 29.1, 37.7, 39.0, 42.1 (Ad), 96.7 (CO), 114.4 (C=C), 149.8 (C=C); ^{29}Si NMR δ (C_6D_6) −8.5, −7.7, 7.6.

3.4. Reaction of **1** with acrolein at 120 °C

A mixture of compound **1** (0.0998 g, 0.265 mmol) and 0.0962 g (1.72 mmol) of acrolein was heated in a sealed tube at 140 °C for 12 h. Product **5** (0.0534 g, 47% isolated yield) and the starting compound **1** (0.0225 g, 22%) were isolated by column chromatography. For **5**: Anal. Calcd for $C_{17}H_{40}O_2Si_3Ge$: C, 47.12; H, 9.30. Found: C, 47.10; H, 9.22. MS m/z 434 (M^+); ^{1}H NMR δ (C_6D_6) 0.24 (s, 9H, Me_3Si), 0.27 (s, 9H, Me_3Si), 0.29 (s, 9H, Me_3Si), 1.08 (s, 9H, t-Bu), 1.30 (dd, 1H, CH_2, J = 16.0 Hz, 7.3 Hz,), 1.71 (dt, 1H, CH_2, J = 16.0 Hz, 2.5 Hz), 4.76 (dt, 1H, olefinic proton, J = 7.3 Hz, 2.5 Hz), 6.02 (dd, 1H, olefinic proton, J = 7.3 Hz, 2.5 Hz); ^{13}C NMR δ (C_6D_6) 0.6, 1.1, 2.4 (Me_3Si), 3.7 (CH_2Ge), 26.7 (Me_3C), 40.6 (CMe_3), 101.8 (C=C), 112.8 (CO), 143.8 (C=C); ^{29}Si NMR δ (C_6D_6) −8.2, −7.7, 8.4.

3.5. Reaction of **2** with acrolein at 120 °C

A mixture of compound **2** (0.1093 g, 0.240 mmol) and 0.0746 g (1.33 mmol) of acrolein was heated in a sealed tube at 140 °C for 12 h. Product **6** (0.0703 g, 57% isolated yield) and the starting compound **2** (0.0080 g, 7% isolated yield) were isolated by column chromatography. For **6**: Anal. Calcd for $C_{23}H_{46}O_2Si_3Ge$: C, 54.01; H, 9.06. Found: C, 53.88; H, 9.01. Mp. 67–69 °C; MS m/z 512 (M^+); ^{1}H NMR δ (C_6D_6) 0.26 (s, 9H, Me_3Si), 0.31 (s, 9H, Me_3Si), 0.32 (s, 9H, Me_3Si), 1.29 (dd, 1H, CH_2, J = 16.0 Hz, 7.4 Hz), 1.69–2.03 (m, 16H, Ad, CH_2), 4.77 (dt, 1H, olefinic proton, J = 7.4 Hz, 2.2 Hz), 6.03 (dd, 1H, olefinic proton, J = 7.4 Hz, 2.9 Hz); ^{13}C NMR δ (C_6D_6) 0.7, 1.2, 2.5 (Me_3Si), 3.5 (CH_2Ge), 29.0, 37.7, 38.8, 42.1 (Ad), 101.9 (C=C), 114.0 (CO), 143.7 (C=C); ^{29}Si NMR δ (C_6D_6) −8.2, −7.6, 8.5.

3.6. Reaction of **1** with methyl vinyl ketone at 130 °C

A mixture of compound **1** (0.1040 g, 0.276 mmol) and 0.1176 g (1.68 mmol) of methyl vinyl ketone was heated in a sealed tube at 130 °C for 12 h. Products **3** (0.0354 g, 29% isolated yield) and **7** (0.0227 g, 18% isolated yield) were isolated by column chromatography. For **7**: Exact Mass Calcd for $C_{18}H_{42}O_2Si_3Ge$ ([M^+]) 448.1704, Found 448.1727. MS m/z 448 (M^+); ^{1}H NMR δ (C_6D_6) 0.18 (s, 9H, Me_3Si), 0.32 (s, 18H, Me_3Si), 1.04 (s, 9H, t-Bu), 1.68 (s, 3H, Me), 2.28 (d, 2H, CH_2, J = 8.3 Hz), 4.69 (t, 1H, olefinic proton, J = 8.3 Hz); ^{13}C NMR δ (C_6D_6) 0.9, 1.0 (Me_3Si), 12.3 (CH_2Ge), 22.8 (Me), 24.9 (Me_3C), 49.4 (CMe_3), 107.7, 144.4 (C=C), 244.9 (CO); ^{29}Si NMR δ (C_6D_6) −6.6, 15.3. All spectral data for **3** were identical with those of the authentic samples described above.

3.7. Reaction of **2** with methyl vinyl ketone at 130 °C

A mixture of compound **2** (0.1283 g, 0.282 mmol) and 0.0725 g (1.03 mmol) of methyl vinyl ketone was heated in a sealed tube at 130 °C for 12 h. Products **4** (0.0346 g, 23% isolated yield) and **8** (0.0332 g, 22%) were isolated by column chromatography. For **8**: Exact Mass Calcd for $C_{24}H_{48}O_2Si_3Ge$ ([M^+]) 526.2179, Found 526.2164. MS m/z 526 (M^+); ^{1}H NMR δ (C_6D_6) 0.18 (s, 9H, Me_3Si), 0.36 (s, 18H, Me_3Si), 1.58–1.63 (m, 6H, Ad), 1.69 (s, 3H, Me), 1.83–1.84 (m, 6H, Ad), 1.94 (br s, 3H, Ad), 2.33 (d, 2H, CH_2, J = 8.3 Hz), 4.75 (t, 1H, olefinic proton, J = 8.3 Hz); ^{13}C NMR δ (C_6D_6) 0.9, 1.1 (Me_3Si), 12.3 (CH_2Ge), 22.8 (Me), 28.6, 37.1, 37.5, 52.0 (Ad), 108.0, 144.3 (C=C), 245.3 (CO); ^{29}Si NMR δ (C_6D_6) −6.7, 15.3. All spectral data for **4** were identical with those of the authentic samples described above.

3.8. Reaction of **1** with acrolein at 130 °C

A mixture of compound **1** (0.1059 g, 0.281 mmol) and 0.0336 g (0.599 mmol) of acrolein was heated in a sealed tube at 130 °C for 12 h. Products **5** (0.0217 g, 18% isolated yield) and **9** (0.0276 g, 23%) were isolated by column chromatography. For **9**: Exact Mass Calcd for $C_{17}H_{40}O_2Si_3Ge$ ([M^+]) 434.1551, Found 434.1552. MS m/z 434 (M^+); ^{1}H NMR δ (C_6D_6) 0.10 (s, 9H, Me_3Si), 0.32 (s, 18H, Me_3Si), 1.03 (s, 9H, t-Bu), 2.42 (dd, 2H, CH_2, J = 8.6 Hz, 1.6 Hz), 4.79 (dt, 1H, olefinic proton, J = 8.6 Hz, 5.8 Hz), 6.01 (dt, 1H, olefinic proton, J = 5.8 Hz, 1.6 Hz); ^{13}C NMR δ (C_6D_6) −0.5, 1.0 (Me_3Si), 10.6 (CH_2Ge), 25.0 (Me_3C), 49.4 (CMe_3), 110.1, 136.0 (C=C), 244.8 (CO); ^{29}Si NMR δ (C_6D_6) −6.4, 19.7. All spectral data for **5** were identical with those of the authentic samples described above.

3.9. Reaction of **2** with acrolein at 130 °C

A mixture of compound **2** (0.1052 g, 0.231 mmol) and 0.0582 g (1.04 mmol) of acrolein was heated in a sealed tube at 130 °C for 12 h. Product **6** (0.0264 g, 22% isolated yield) and **10** (0.0382 g, 32% isolated yield) were isolated by column chromatography. For **10**: Exact Mass Calcd for $C_{23}H_{46}O_2Si_3Ge$ ([M^+]) 512.2022, Found 512.2026. MS m/z 512 (M^+); ^{1}H NMR δ (C_6D_6) 0.10 (s, 9H, Me_3Si), 0.36 (s, 18H, Me_3Si), 1.58–1.61 (m, 6H, Ad), 1.82–1.84 (m, 6H, Ad), 1.92 (br s, 3H, Ad), 2.47 (dd, 2H, CH_2, J = 8.6 Hz, 1.3 Hz), 4.84 (dt, 1H,

olefinic proton, J = 8.6 Hz, 5.9 Hz), 6.03 (dt, 1H, ring proton, J = 5.9 Hz, 1.3 Hz); ^{13}C NMR δ (C_6D_6) −0.5, 1.2 (Me_3Si), 10.6 (CH_2Ge), 28.5, 37.1, 37.5, 52.0 (Ad), 110.4, 135.9 (C═C), 245.1 (CO); ^{29}Si NMR δ (C_6D_6) −6.5, 19.6. All spectral data for **6** were identical with those of the authentic samples described above.

3.10. Reaction of **1** with methyl vinyl ketone at 140 °C

A mixture of compound **1** (0.1100 g, 0.292 mmol) and 0.0520 g (0.742 mmol) of methyl vinyl ketone was heated in a sealed tube at 140 °C for 12 h. Product **7** (0.1210 g, 41% isolated yield) was isolated by column chromatography. All spectral data for **7** were identical with those of the authentic sample described above.

3.11. Reaction of **2** with methyl vinyl ketone at 140 °C

A mixture of compound **2** (0.1260 g, 0.277 mmol) and 0.1191 g (1.70 mmol) of methyl vinyl ketone was heated in a sealed tube at 140 °C for 12 h. Products **4** (0.0051 g, 4% isolated yield) and **8** (0.0420 g, 29% isolated yield) were isolated by column chromatography. All spectral data for **4** and **8** were identical with those of the authentic samples described above.

3.12. Reaction of **1** with acrolein at 140 °C

A mixture of compound **1** (0.1035 g, 0.274 mmol) and 0.0659 g (1.18 mmol) of acrolein was heated in a sealed tube at 140 °C for 12 h. Products **5** (0.0059 g, 5% isolated yield) and **9** (0.0281 g, 24% isolated yield) were isolated by column chromatography. All spectral data for **5** and **9** were identical with those of the authentic samples described above.

3.13. Reaction of **2** with acrolein at 140 °C

A mixture of compound **2** (0.1071 g, 0.235 mmol) and 0.0504 g (0.899 mmol) of acrolein was heated in a sealed tube at 140 °C for 12 h. Product **6** (0.0113 g, 11% isolated yield) and **10** (0.0404 g, 34% isolated yield) were isolated by column chromatography. All spectral data for **6** and **10** were identical with those of the authentic samples described above.

3.14. Reaction of **3** at 140 °C

Compound **3** (0.0816 g, 0.182 mmol) in a sealed glass tube was heated at 140 °C for 12 h. Product **7** (0.0353 g, 43% isolated yield) was isolated by column chromatography. All spectral data for **7** were identical with those of the authentic sample described above.

3.15. Reaction of **7** with 2,3-dimethyl-1,3-butadiene at 140 °C

A mixture of compound 7 (0.0779 g, 0.174 mmol) and 0.0787 g (0.958 mmol) of 2,3-dimethyl-1,3-butadiene was heated in a sealed tube at 140 °C for 12 h. Products **11** and **12** (0.0849 g, 92% isolated yield) were isolated by column chromatography. The ratio of **11** and **12** was calculated to be 1:1 by the ^{1}H NMR spectrometric analysis. For **11** and **12**: Exact Mass Calcd for $C_{24}H_{52}O_2Si_3Ge$ ([M^+]) 530.2492, Found 530.2515. MS m/z 530 (M^+); ^{1}H NMR δ (C_6D_6) 0.18 (s, 9H, Me_3Si), 0.20 (s, 9H, Me_3Si), 0.23 (s, 9H, Me_3Si), 0.25 (s, 9H, Me_3Si), 0.28 (s, 9H, Me_3Si), 0.29 (s, 9H, Me_3Si), 1.05 (s, 9H, t-Bu), 1.12 (s, 9H, t-Bu), 1.53 (d, 1H, CH_2, J = 16.0 Hz), 1.63 (s, 3H, Me), 1.70 (s, 3H, Me), 1.76 (s, 3H, Me), 1.79 (s, 6H, Me), 1.81 (s, 3H, Me), 1.88−2.17 (m, 9H, CH_2), 2.30 (d, 1H, CH_2, J = 17.1 Hz), 2.42 (d, 1H, CH_2, J = 17.1 Hz), 4.47 (t, 1H, olefinic proton, J = 8.2 Hz), 4.68 (t, 1H, olefinic proton, J = 8.2 Hz); ^{13}C NMR δ (C_6D_6) 0.3, 1.0 (2C), 2.3, 3.1 (2C) (Me_3Si), 13.4 (2C), 18.0, 18.7 (CH_2Ge), 19.5, 19.6, 21.9, 22.6, 22.9, 23.8 (Me), 27.6, 29.4 (Me_3C), 39.5, 40.6 (CMe_3), 43.6 (2C) (CH_2), 85.1, 86.9 (CO), 105.0, 106.9 (HC = C), 125.1, 128.2, 131.1, 131.2, 144.4, 145.2 (C═C); ^{29}Si NMR δ (C_6D_6) 1.0, 3.9, 4.2, 14.6.

Acknowledgment

We express our appreciation to Shin-Etsu Co., Ltd. for a gift of organochlorosilanes.

References

[1] V.Y. Lee, A. Sekiguchi, Organometallics 23 (2004) 2822.
[2] N. Tokitoh, R. Okazaki, in: Z. Rappoport (Ed.), The Chemistry of Organic Germanium, Tin, and Lead Compounds, vol. 2, Wiley, New York, 2002 Chapter 13.
[3] (a) J. Escudié, H. Ranaivonjatovo, Adv. Organomet. Chem. 44 (1999) 113; (b) J. Escudié, C. Couret, H. Ranaivonjatovo, Coord. Chem. Rev. 178–180 (1998) 565.
[4] W.J. Leigh, Pure. Appl. Chem. 71 (1999) 453.
[5] K.M. Baines, W.G. Stibbs, Adv. Organomet. Chem. 39 (1996) 275.
[6] (a) J. Barrau, J. Escudié, J. Satgé, Chem. Rev. 90 (1990) 283; (b) J. Satgé, Pure. Appl. Chem. 56 (1984) 137; (c) J. Satgé, Adv. Organomet. Chem. 21 (1982) 241.
[7] N. Wiberg, J. Organomet. Chem. 273 (1984) 141.
[8] H. Meyer, G. Baum, W. Massa, A. Berndt, Angew. Chem. Int. Ed. Engl. 26 (1987) 798.
[9] H. Schumann, M. Glanz, F. Girgsdies, F.E. Hahn, M. Tamm, A. Grzegorzewski, Angew. Chem. Int. Ed. Engl. 36 (1997) 2232.
[10] D. Bravo-Zhivotovskii, I. Zharov, M. Kapon, Y. Apeloig, J. Chem. Soc. Chem. Commun. (1995) 1625.
[11] N.P. Toltl, W.J. Leigh, J. Am. Chem. Soc. 120 (1998) 1172.
[12] V.N. Khabashesku, K.N. Kudin, J. Tamás, S.E. Boganov, J.L. Margrave, O. M. Nefedov, J. Am. Chem. Soc. 120 (1998) 5005.
[13] M.A. Chaubon, J. Escudié, H. Ranaivonjatovo, J. Satgé, J. Chem. Soc., Dalton Trans. (1996) 893.
[14] (a) D. Ghereg, S. Ech-Cherif El Kettani, M. Lazraq, H. Ranaivonjatovo, W. W. Schoeller, J. Escudié, H. Gornitzka, Chem. Commun. (2009) 4821; (b) S. Ech-Cherif El Kettani, M. Lazraq, F. Ouhsaine, H. Gornitzka, H. Ranaivonjatovo, J. Escudié, Org. Biomol. Chem. 6 (2008) 4064; (c) S. Ech-Cherif El Kettani, J. Escudié, C. Couret, H. Ranaivonjatovo, M. Lazraq, M. Soufiaoui, H. Gornitzka, G.C. Nemes, Chem. Commun. (2003) 1662; (d) C. Couret, J. Escudié, G. Delpon-Lacaze, J. Satgé, Organometallics 11 (1992) 3176; (e) G. Anselme, J. Escudié, C. Couret, J. Satgé, J. Organomet. Chem. 403 (1991) 93; (f) C. Couret, J. Escudié, J. Satgé, M. Lazraq, J. Am. Chem. Soc. 109 (1987) 4411.
[15] (a) N. Wiberg, H.-S. Hwang-Park, J. Organomet. Chem. 519 (1996) 107; (b) N. Wiberg, H.-S. Hwang-Park, P. Mikulcik, G. Müller, J. Organomet. Chem. 511 (1996) 239.
[16] F. Meiners, D. Haase, R. Koch, W. Saak, M. Weidenbrüch, Organometallics 21 (2002) 3990.
[17] N. Wiberg, C.K. Kim, Chem. Ber. 119 (1986) 2980.
[18] M. Lazraq, C. Couret, J. Escudié, J. Satgé, Organometallics 10 (1991) 1771.
[19] S. Ech-Cherif El Kettani, M. Lazraq, H. Ranaivonjatovo, J. Escudié, C. Couret, H. Gornitzka, A. Atmani, Organometallics 24 (2005) 5364.
[20] N.J. Mosey, K.M. Baines, T.K. Woo, J. Am. Chem. Soc. 124 (2002) 13306.
[21] (a) M. Lazraq, J. Escudié, C. Couret, J. Satgé, Organometallics 11 (1992) 555; (b) S. Eh-Cherif El Kettani, M. Lazraq, H. Ranaivonjatovo, J. Escudié, H. Gornitzka, F. Ouhsaine, Organometallics 26 (2007) 3729.
[22] A. Naka, S. Ueda, M. Ishikawa, J. Organomet. Chem. 692 (2007) 2357.
[23] A. Naka, H. Ohnishi, I. Miyahara, K. Hirotsu, Y. Shiota, K. Yoshizawa, M. Ishikawa, Organometallics 23 (2004) 4277.
[24] (a) K.K. Milnes, M.C. Jennings, K.M. Baines, J. Am. Chem. Soc. 128 (2006) 2491; (b) K.K. Milnes, M.C. Jennings, K.M. Baines, Organometallics 26 (2007) 2392.
[25] A.G. Brook, S.S. Hu, W.J. Chatterton, A.J. Lough, Organometallics 10 (1991) 2752.
[26] K. Fukui, Acc. Chem. Res. 14 (1981) 363.
[27] A.D. Becke, J. Chem. Phys. 98 (1993) 1372.
[28] P.M.W. Gill, B.G. Johnson, J.A. Pople, Int. J. Quantum Chem. Symp. 26 (1992) 319.
[29] M.J. Frisch, G.W. Trucks, H.B. Schlegel, G.E. Scuseria, M.A. Robb, J. R. Cheeseman, J.A. Montgomery Jr., T. Vreven, K.N. Kudin, J.C. Burant, J. M. Millam, S.S. Iyengar, J. Tomasi, V. Barone, B. Mennucci, M. Cossi, G. Scalmani, N. Rega, G.A. Petersson, H. Nakatsuji, M. Hada, M. Ehara, K. Toyota, R. Fukuda, J. Hasegawa, M. Ishida, T. Nakajima, Y. Honda, O. Kitao, H. Nakai, M. Klene, X. Li, J.E. Knox, H.P. Hratchian, J.B. Cross, V. Bakken, C. Adamo, J. Jaramillo, R. Gomperts, R.E. Stratmann, O. Yazyev, A.J. Austin, R. Cammi, C. Pomelli, J.W. Ochterski, P.Y. Ayala, K. Morokuma, G.A. Voth, P. Salvador, J.J. Dannenberg, V.G. Zakrzewski, S. Dapprich, A.D. Daniels, M. C. Strain, O. Farkas, D.K. Malick, A.D. Rabuck, K. Raghavachari, J.B. Foresman, J. V. Ortiz, Q. Cui, A.G. Baboul, S. Clifford, J. Cioslowski, B.B. Stefanov, G. Liu, A. Liashenko, P. Piskorz, I. Komaromi, R.L. Martin, D.J. Fox, T. Keith, M.A. Al-Laham, C.Y. Peng, A. Nanayakkara, M. Challacombe, P.M.W. Gill, B. Johnson, W. Chen, M.W. Wong, C. Gonzalez, J.A. Pople, Gaussian 03, Revision B.03. Gaussian, Inc., Pittsburgh PA, 2003.